

## Wavelet-Based and Database Approach for Locating Faulty Section of High Impedance Fault in a Distribution System

**Abstract.** Locating a faulty section of the high impedance fault (HIF) in a power system network is a major challenge especially for a distribution network. This is due to the effect of the complexity of the distribution network such as branches, non-homogenous lines and high fault impedance that results in variation of fault locations. In this paper, analysis of fault locations using Discrete Wavelet Transform-based Multi-Resolution Analysis (MRA) has been proposed. A three-phase voltage signal measured at the main substation is analyzed to locate the high impedance fault. The 1<sup>st</sup>, 2<sup>nd</sup> and 3<sup>rd</sup> levels of detailed coefficient resolution for each phase were used for the classification of fault locations using the proposed method. The simulation was conducted on a 38-node distribution network system in a national grid in Malaysia using PSCAD software. The proposed method has successfully determined the actual fault location of a high impedance fault.

**Streszczenie.** W artykule przedstawiono analizę metody lokalizacji awarii w sieci energetycznej, wykorzystującej analizę wielo-wynikową (ang. Multiresolution Analysis), opartą na dyskretnej transformacji falkowej. Analizie poddawany jest sygnał pomiarowy napięcia trójfazowego w podstacji. Przeprowadzono badania symulacyjne w programie PSCAD na systemie dystrybucji energii elektrycznej o 38 korzeniach w malezyjskich państwowych sieciach energetycznych. (Lokalizacja awaryjnej sekcji w przypadku awarii izolatora w sieci dystrybucji energii elektrycznej – wykorzystanie analizy danych i transformacji falkowej).

**Keywords:** Discrete Wavelet Transform-based MRA, Faulty section, High Impedance Fault.

**Słowa kluczowe:** MRA z dyskretną transformacją falkową, awaryjna sekcja, awaria izolatora.

### Introduction

High impedance fault (HIF) is a phenomenon when there is an undesirable electrical contact between a conductor and non-conducting or poor conductivity object or surface. Normally, HIF occurred when a conductor physically breaks and touches high impedance surfaces. It can also happen when the conductor is not broken but comes in contact with non-grounded objects, either through a failure of the conductor mounting system, unintentional contact with any external non-conducting element or insulation failure. This type of HIF fault also exhibits the same arcing signature as a broken conductor lying on the ground. This arcing scenario may lead to potential hazards to both human life and the environment. Fire hazard may also occur due to the arcing phenomenon that is associated with HIF. Since HIF occurrence is dangerous, utility companies must detect and locate it as fast as possible. Therefore, a reliable detection scheme is needed to detect high impedance faults in a distribution system.

There have been a lot of HIF detection schemes proposed [7-10], where most of the detection schemes focus on identifying special features of the voltage and current signals associated with HIF. In order to extract useful features from these voltage and current signals, some signal processing methods have been utilized, such as Modal Analysis, Fourier Transform, Prony Analysis, Discrete Wavelet Transform, S-Transform, TT-Transform, Phase Space Reconstruction and Mathematical Morphology [1],[3-8],[10],[18-22].

Wavelet Transform has been widely used in power quality analysis [1]-[6]. In general, discrete wavelet transforms (DWT) is widely utilized because of its capability to extract important information such as the abrupt changing feature of the signal and locating the frequency features of the signal in time-domain. Wenzhong and Jiaxin have used a wavelet-based method to obtain the characteristics of frequency and voltage derivative for disturbance analysis of generation loss and load changes [6].

For the high impedance fault detection, the important features are extracted from voltage and current signals. Irregularities in the voltage and current waveforms will produce patterns of unique characteristics. In [7-9], DWT

has been used to extract the features of the voltage and current signals during HIF event. Sarlak and Shahrtash employed a multi-resolution morphological gradient (MMG) for feature extraction of the current waveform [10]. They had also used the MMG method to distinguish HIF event from other phenomena such as capacitor bank switching, load switching and harmonic load.

Even though HIF can be detected as mentioned in [7-10], locating the fault is the most challenging part. Identifying or estimating the exact fault location is necessary so that power restoration can be expedited and thus reducing the outage time and considerably improving the system reliability. In [11-13], [23], different approaches and various criteria were discussed for fault locating on distribution network. Some of the strategies used are impedance based method, fundamental voltage and current based method, travelling wave based method, topology-based method and knowledge-based method. The advantages and disadvantages for each method were discussed and the comparison between all methods was made.

Nagy *et al.* used the DWT to extract the voltage and current residuals to identify a faulty feeder [14]. The faulty feeder was determined based on the power polarity. DWT detailed coefficients for phase voltage and current were multiplied for each feeder and the faulty feeder was detected if the power polarity is negative. In another work, Nagy *et al.* used the ratio of the residual current amplitude method to determine the faulty feeder [15]. Wireless sensor was placed at the end of each node to measure the feeder line current. The ratio of the residual current amplitude was computed between the fundamental components of each section with respect to the parent section. The highest ratio of the measured residual current amplitude determines the faulty feeder.

For the classification of faulty sections, Dwivedi *et al.* determined the faulty section by comparing the sharp variation value of the detailed signal at each section [16]. They utilized the summation of 3<sup>rd</sup> level detailed coefficient of a current signal.

A topology method has been proposed to identify the faulty section [17]. Voltage signal is measured to determine the active sensor. The 'active sensor' located within the

faulty region gives increment of the relative voltage difference. The faulty section is identified based on the last two nodes of a common 'active sensor' path. Even though this method can determine a faulty section easily, voltage sensor is required at each end of the feeder.

In this work, classification of the faulty section in a complex distribution network using discrete wavelet transform-based multi-resolution analysis and a database approach is proposed. The proposed method uses only three-phase voltage signal measured at the primary substation. It utilizes the 1<sup>st</sup>, 2<sup>nd</sup> and 3<sup>rd</sup> level resolutions of detailed coefficients that are obtained from the wavelet multi-resolution decomposition. Average method is developed to set the databases and the ranking process to determine the faulty section. The proposed fault location method has been tested on a typical 11kV distribution network system in Malaysia. The simulation results were compared with the actual data to validate the proposed method.

### Discrete Wavelet Transform-Based Multi-Resolution Analysis of a Fault Signal

Wavelet is a mathematical function that satisfies certain mathematical requirements to represent the signal in time domain. The fundamental idea behind this is to analyze the signal according to scale, by dilation and translation. Referring to Fig. 1, the translation and dilation operations are performed to obtain the wavelet coefficients to represent the wavelet correlation to the signal.

Discrete wavelet transforms (DWT)-based Multi-Resolution Analysis (MRA) is the extension of the DWT where the decomposition process is iterated with successive approximation components. DWT-based MRA splits the analyzed signal into many lower resolution levels until the individual detailed component consists of a single sample.

Using discrete wavelet transform (DWT) - based Multi-Resolution Analysis (MRA), wavelet coefficients are calculated based on the subset of scales and positions. The scales and positions are chosen based on the power of two, called *dyadic* scales and positions. In DWT, the original signal is decomposed by two complementary filters (high-pass and low-pass filters) and emerges as two signals (high-frequency and low-frequency components). The low-frequency components of the signal are high-scaled decomposition, called *approximations*. The high-frequency component is low-scale decomposition, known as *details*.

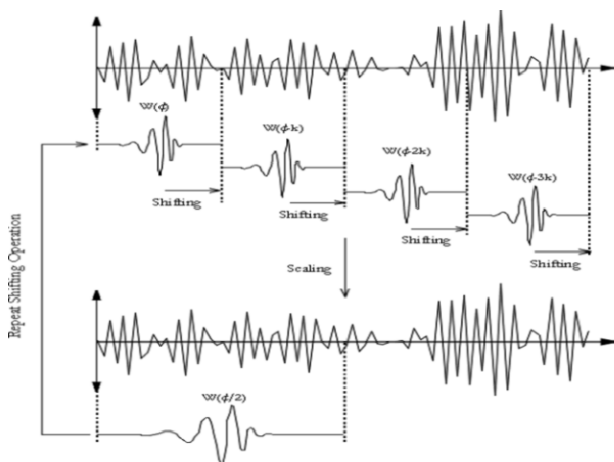


Fig.1. Shifting (translation) and scaling (dilation) process of the mother wavelet

DWT-based MRA is a decomposition process that can be iterated with successive approximations to obtain more

resolution levels. Fig. 2 shows the implementation of DWT-based MRA by using a bank of high pass filters, H and a low pass filters, L. The input signal, S, which propagates through the high pass and low pass filters is decomposed into low-pass component,  $c_m$  and high-pass component,  $d_m$  at each stage, where  $m=1, 2, \dots, j$ . The scaling coefficients,  $c_m$  represent the approximation of the low-pass signal information and wavelet coefficients and  $d_m$  represents the detailed high-pass signal information.

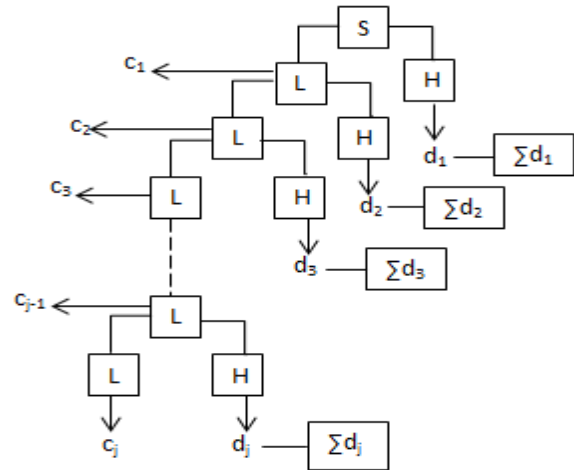


Fig.2. Discrete wavelet transform-based Multi-Resolution Analysis of a faulted signal.

Information extracted from the signal using DWT-based MRA is used to detect and identify various types of faults and to locate the faulty section in a distribution system network. To locate the faulty section, unique and useful information of voltage signals obtained can be analyzed using DWT-based MRA. Various patterns of voltage signal are obtained for different faulty section.

### Proposed Method for the High Impedance Fault Location

In this paper, the classification of high impedance fault location algorithm is constructed based on the wavelet database. This section describes a tested distribution network, fault detection and classification, wavelet-based database development and ranking analysis.

#### Fault Detection & Classification

For high impedance fault (HIF) detection and classification of fault location, 2 cycles of post-disturbance of voltage signal is analyzed. Discrete wavelet transforms of Daubechies 4<sup>th</sup> order, Daub4 is used to observe the voltage signal.

HIF is detected when the detailed coefficient surge gives the higher instantaneous fluctuation. This provides an easy means to identify an abnormality in the voltage signal as shown in Fig. 4(d). In order to classify the faulty section, the 1<sup>st</sup>, 2<sup>nd</sup> and 3<sup>rd</sup> level of the detailed signal of dB4 are analyzed and their summations of detailed coefficients are measured.

#### Extracted Data for Database Development

To generate a set of database, several high impedance faults (HIF) such as 60Ω, 70Ω, 80Ω, 90Ω and 100Ω fault impedance are simulated at each node. The voltage signal obtained from the main feeder is decomposed using the DWT-based MRA to obtain the value of detailed coefficients for 2 cycles of post-disturbance event. Experimentally, it has been found that different fault impedances generate unique patterns of detailed coefficients at each node. The average detailed coefficient,  $A_v$  between two neighboring nodes is calculated and stored in a database for the

particular section between the two nodes.  $A_v$  is calculated using:

$$(1) \quad A_v = \frac{\sum d_i + \sum d_j}{2}$$

where:  $A_v$  - Average detailed coefficients between two nodes for phase A, B and C;  $\sum d_i$  - Summation of detailed coefficients for levels 1, 2 and 3 for nodes  $i$ ;  $\sum d_j$  - Summation of detailed coefficients for levels 1, 2 and 3 for node  $j$ ;  $i$  and  $j$  is two adjacent nodes.

A list of all sections between two neighboring nodes is shown in the Appendix section. There are 5 sets of databases, which are for 60Ω, 70Ω, 80Ω, 90Ω and 100Ω fault impedance values. Each database for one section consists of 18 data of the 1<sup>st</sup>, 2<sup>nd</sup> and 3<sup>rd</sup> levels of detailed coefficients for phases A, B and C of the 1<sup>st</sup> and 2<sup>nd</sup> cycles of post-disturbance voltage waveform.

The steps of creating the database are shown as follows:

- 1) Fault on each node, starting from node 1 to node  $N$  is generated (where  $N$  is the total number of nodes).
- 2) The first and second cycles of post-disturbance voltage waveform are analyzed. The first cycle of post-disturbance is determined from the sharp fluctuation of the detailed signal.
- 3) DWT-based MRA is performed.
- 4) The first, second and third levels of detailed coefficients for each phase are determined.
- 5) The data are stored in a database.
- 6) Step 1 – 5 is repeated for all nodes.
- 7) The averages of summation of detailed coefficients,  $A_v$  are calculated between nodes  $i$  and node  $j$  ( $i$  and  $j$  is two adjacent nodes).
- 8)  $A_v$  is stored in the database for a particular line section of node  $i$ - $j$ .
- 9) The value of  $j$  is checked. If  $j$  is not equal to  $N$ , step 7-8 is repeated.
- 10) If  $j$  is equal to  $N$ , the process is terminated.

The process is continued until a database for each section is obtained.

### Ranking Analysis

The main objective of this work is to locate the faulty section. This is obtained by calculating the *average of absolute difference* (AAD) between the faulty signal and database using

$$(2) \quad ADD = \frac{\sum_{i=1}^n |\sum d_{i(measured)} - A_v|}{n}$$

where:  $n$  – number of data, i.e.  $n=18$

The faulty section is determined by finding the smallest value of AAD for all sections. The signal will be compared with all five databases for each section. Then, the ranking is made from the lowest to the highest value of AAD. This is done because in some cases, there will be error in locating the faulty section from the first ranked due to the complexity of a distribution network. This is due to the influence of branches and non-homogenous line that results in variation of faulty location. Thus, the second lowest AAD value will be considered as a faulty section until the real faulty section is traced.

### Simulation and Results

A schematic diagram of a typical 11kV distribution network system in Malaysia consists of 38 nodes, as shown in Fig. 3, is used as the test system. The system frequency

is 50Hz and the sampling frequency is 6.4 kHz, which produces 128 data samples for each cycle. The measurement is taken at a feeder bus from a 132/11kV radial distribution network. The line data of this network are shown in the Appendix section.

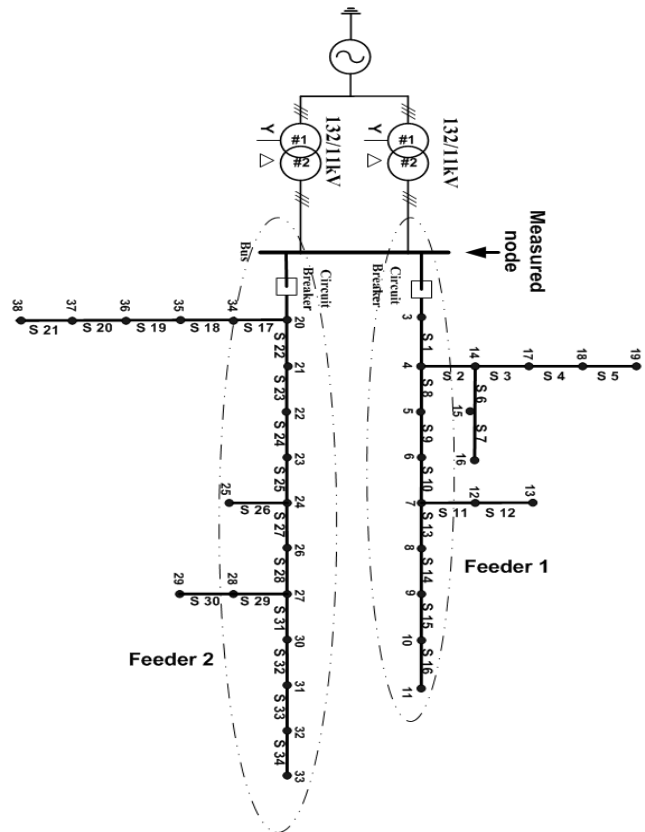


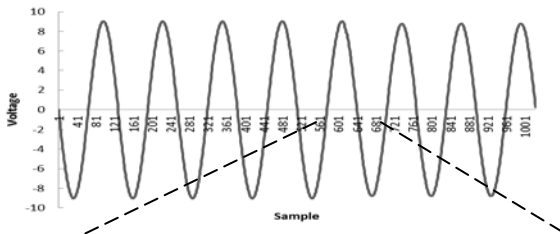
Fig.3. Schematic diagram of a distribution network in Malaysia.

The simulation has been performed to create a database and the proposed algorithm is tested with different values of high impedance fault of SLGF. This type of fault is considered since it is the most frequent type of fault occurs in a distribution system. The simulation was carried out using the PSCAD software to obtain the voltage of the faulty signal. The voltage was analyzed using wavelet transform in MATLAB.  $A_v$  was calculated and the ranking for all sections based on the value of AAD was determined.

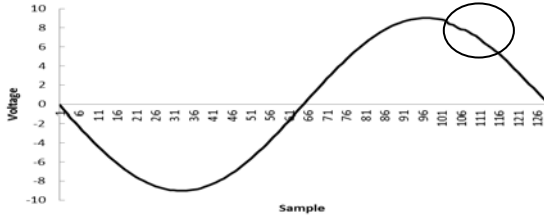
### Wavelet Waveform Analysis

To investigate the effectiveness of the proposed algorithm, different fault impedances from the database are tested. The tested fault impedances are 75Ω, 85Ω and 95Ω. The fault was applied in the middle of the line section. After the fault was applied, there was a small fluctuation in the voltage signal. However, the fluctuation was hardly seen as shown in Fig. 4(a). After the image was expanded as shown in Fig. 4(b) and Fig. 4(c), a small deviation can be seen clearly on the signal.

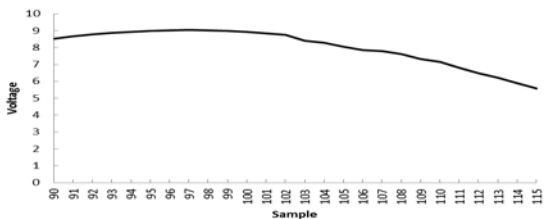
In the previous method of detecting high impedance fault such as impedance-based method, this small deviation cannot be detected since it acts like a normal signal. Thus, in order to better illustrate the anomaly in the signal, a digital signal processing technique is used in this work to analyze the signal. Wavelet transform was applied to examine the signal content. After the signal was decomposed using the DWT-based MRA, sharp fluctuations in the detailed signal can be seen, as shown in Fig. 4 (d). This sharp variation depicts the time when the fault occurred.



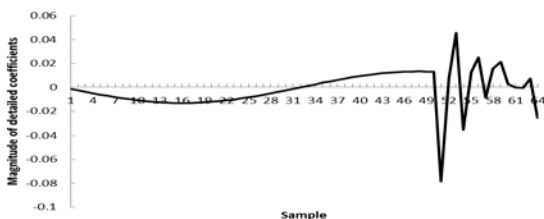
(a). Instantaneous voltage signal



(b). 1<sup>st</sup> cycle of post-fault



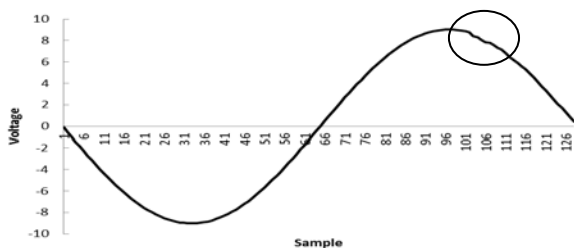
(c). Zooming in the fluctuation



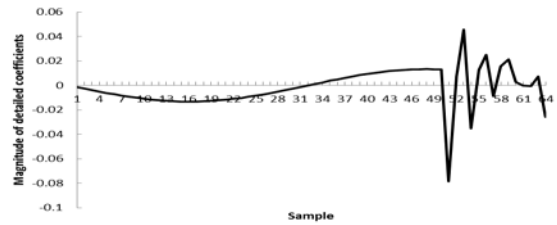
(d). Detailed coefficients of wavelet transform  
Fig.4. HIF detection of a voltage signal.

Fig. 5(a) and Fig. 6(a) show the first and second cycles of post-disturbance voltage signal respectively. The fault happens in the middle of section 1 with 75Ω fault impedance. Both of the cycles are analyzed using the DWT-based MRA. After the signal is decomposed, the 1<sup>st</sup>, 2<sup>nd</sup> and 3<sup>rd</sup> level of the detailed signal are obtained, as shown in Fig. 5(b)-5(d) and Fig. 6(b)-6(d).

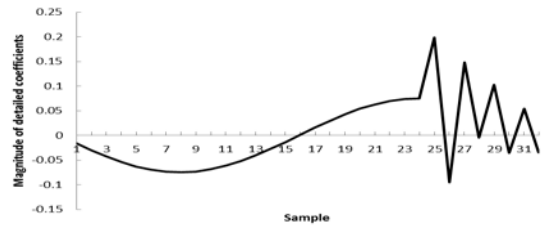
The 1<sup>st</sup> level consists of 64 detailed coefficients sampled at 1.6-3.2 kHz frequency range. The 2<sup>nd</sup> and 3<sup>rd</sup> levels consist of 32 and 16 detailed coefficients sampled at 0.8-1.6kHz and 0.4-0.8kHz frequency ranges respectively. These detailed coefficients are summed up for each level and are used for locating the faulty section.



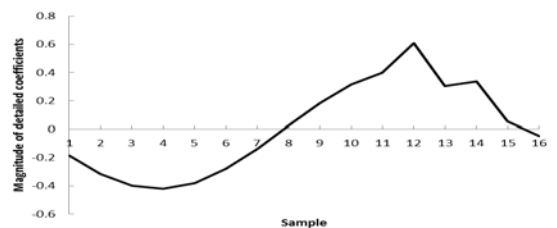
(a). 1<sup>st</sup> cycle of post-fault voltage signal.



(b). 1<sup>st</sup> level of detailed coefficients. ( $\sum d = 0.016476$ ).



(c). 2<sup>nd</sup> level of detailed coefficients. ( $\sum d = 0.157143$ ).

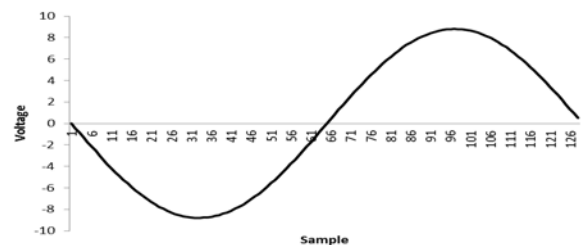


(d). 3<sup>rd</sup> level of detailed coefficients. ( $\sum d = 1.587773$ ).

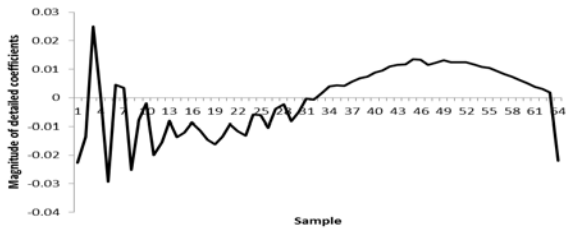
Fig.5. DWT-based MRA analysis for the 1<sup>st</sup> cycle of voltage signal.

The procedures for identifying the faulty section are:

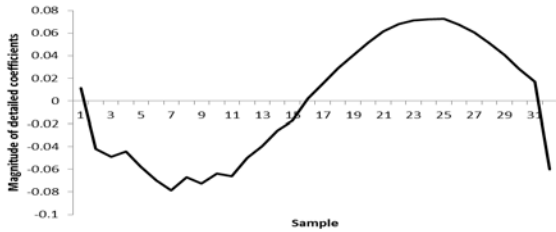
- 1) Data at the measurement point is read.
- 2) The first and second cycles of post-disturbance voltage waveform are analyzed. The first cycle of post-disturbance is determined from the sharp fluctuation of the detailed signal.
- 3) DWT- based MRA is performed.
- 4) The 1<sup>st</sup>, 2<sup>nd</sup> and 3<sup>rd</sup> levels of the detailed coefficients for each phase are determined.
- 5) The average value of absolute difference, AAD between the simulated signal and database is calculated.
- 6) The AAD is ranked from the lowest to highest value, where the lowest value is ranked as #1.
- 7) The faulty section is checked, starting with rank #1.
- 8) If the section of rank #1 is not a faulty section, the faulty section of the next rank is checked. To determine the actual faulty section, a visual inspection by engineers at the faulty location is done.
- 9) The procedure is stopped when the faulty section is located.



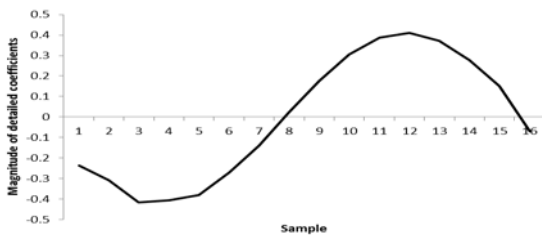
(a). 2<sup>nd</sup> cycle of post-fault voltage signal.



(b). 1<sup>st</sup> level of detailed coefficients. ( $\Sigma d= 0.008644$ ).



(c). 2<sup>nd</sup> level of detailed coefficients. ( $\Sigma d= 0.090403$ ).



(d). 3<sup>rd</sup> level of detailed coefficients. ( $\Sigma d= 1.411884$ ).

Fig.6. DWT-based MRA analysis for the 2<sup>nd</sup> cycle of voltage signal.

Table 1: Test system for different faulty section and fault impedance

Test Section	Fault Impedance
Section 10 (Feeder 1)	75Ω 95Ω
Section 23 (Feeder 2)	85Ω 95Ω
Section 2 (Branch at feeder 1)	75Ω 95Ω
Section 31 (Branch at feeder 2)	85Ω 95Ω

### Analysis of Test Results for Single Line to Ground Fault

Four different locations were selected to show the effectiveness of the method. The location is selected to represent fault at feeder 1, feeder 2 and at the branches. Table 1 summarizes the tested location and fault impedance values. The test results are shown in Table 3 until Table 6

Table 2. Data input of summation of voltage detailed coefficients for fault impedance of 75Ω at section 10

Cycles	LEVEL 1			LEVEL 2			LEVEL 3		
	Phase A	Phase B	Phase C	Phase A	Phase B	Phase C	Phase A	Phase B	Phase C
1 <sup>st</sup> cycle	0.02107	0.01911	0.00907	0.17647	0.12279	0.09931	1.60607	1.43085	1.34539
2 <sup>nd</sup> cycle	0.00796	0.00672	0.00695	0.09027	0.09370	0.09561	1.41283	1.46097	1.48735

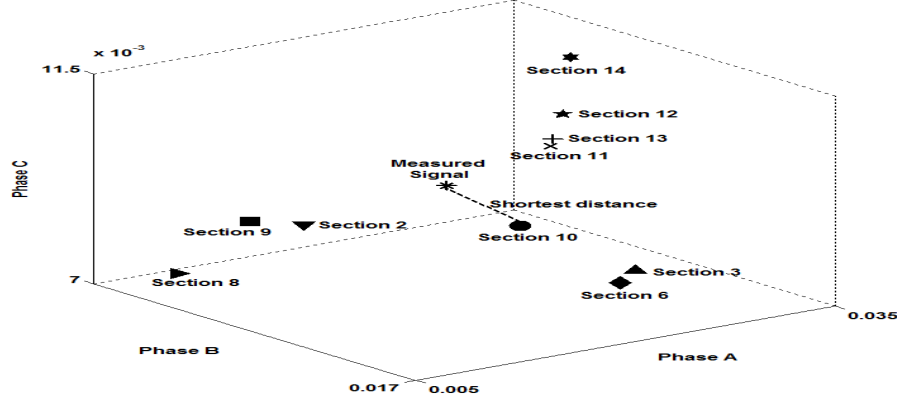


Fig. 7. Three-dimensional view of the closest distance between the measured signal and the expected faulty section

for respective tested section. Each table shows the result for two different fault impedances. The first, second and third columns are the Average of Absolute Difference (AAD), a ranking of the AAD and the faulty section candidate respectively for each fault impedance. By examining the result, the following observation can be seen.

### Test on section 10

The input data that are required to be compared with the databases for each level and phase is shown in Table 2 as an example. This data was generated from the measured voltage at the main substation as shown in Fig. 3. The data of the 1<sup>st</sup> level of summation of detailed coefficients for the 1<sup>st</sup> cycle of voltage signal from Table II is used to find the distance between the measured signal and the expected faulty sections. The section with the closest distance with the measured signal will be selected as the first rank of possible faulty section. Figure 7 shows a three-dimensional view of the measured data and data belong to different sections in the database. It can be observed that section 10 is the closest to the measured data. Hence, section 10 is selected as the first rank of the possible faulty section.

Referring to Table 3, the average of absolute difference, AAD, for each section is calculated. Then, the value of AAD is ranked from the lowest to highest value. For this purpose, only 10 AAD with the smallest value is selected. These rankings give 10 possibilities of the faulty section with rank #1 are the highest possibility. In this case, the fault in the middle of the section 10 with 75Ω and 95Ω fault impedances yields the lowest value of AAD as highlighted (box) in Table 3. These rankings correctly identify the faulty section.

### Test on section 23

For the second test, the fault is tested at the second feeder. For this purpose, section 23 is chosen with 85Ω fault impedance at the middle of the line section. From Table 4, it can be observed that the lowest AAD belongs to section 22 instead of section 23. Since the real fault does not occur in section 22, the next section with the second lowest AAD is checked and it is found that the second lowest AAD belongs to section 23, where the actual fault is located. This is due to the length of section 22 is short (40m), which gives nearly the same voltage characteristic for both section 22 and section 23.

Table 3. Results for fault impedance of 75Ω and 95Ω at section 10

SECTION 10					
75Ω			95Ω		
AAD	Ranking of AAD	Faulty section candidate	AAD	Ranking of AAD	Faulty section candidate
<b>0.00243</b>	<b>1</b>	<b>10</b>	<b>0.00140</b>	<b>1</b>	<b>10</b>
0.00249	2	13	0.00142	2	9
0.00250	3	11	0.00145	3	13
0.00264	4	9	0.00146	4	11
0.00267	5	6	0.00152	5	2
0.00270	6	3	0.00162	6	8
0.00272	7	2	0.00167	7	14
0.00279	8	8	0.00167	8	12
0.00281	9	14	0.00170	9	6
0.00283	10	12	0.00174	10	3

 = correct answer

Table 4. Results for fault impedance of 85Ω and 95Ω at section 23

SECTION 23					
85Ω			95Ω		
AAD	Ranking of AAD	Faulty section candidate	AAD	Ranking of AAD	Faulty section candidate
0.00136	1	22	<b>0.00105</b>	<b>1</b>	<b>23</b>
<b>0.00144</b>	<b>2</b>	<b>23</b>	0.00113	2	22
0.00153	3	17	0.00130	3	17
0.00159	4	19	0.00141	4	19
0.00186	5	23	0.00159	5	24
0.00186	6	24	0.00164	6	18
0.00196	7	18	0.00274	7	25
0.00223	8	22	0.00287	8	20
0.00290	9	17	0.00311	9	21
0.00309	10	25	0.00342	10	26

 = correct answer

Table 5. Results for fault impedance of 75Ω and 95Ω at section 2

SECTION 2					
75Ω			95Ω		
AAD	Ranking of AAD	Faulty section candidate	AAD	Ranking of AAD	Faulty section candidate
<b>0.00246</b>	<b>1</b>	<b>2</b>	0.00141	1	9
0.00251	2	9	<b>0.00144</b>	<b>2</b>	<b>2</b>
0.00258	3	6	0.00156	3	8
0.00262	4	3	0.00158	4	6
0.00265	5	8	0.00161	5	3
0.00272	6	10	0.00164	6	10
0.00292	7	7	0.00179	7	13
0.00296	8	13	0.00180	8	11
0.00298	9	11	0.00181	9	7
0.00303	10	4	0.00193	10	4

 = correct answer

Table 6. Results for fault impedance of 85Ω and 95Ω at section 31

SECTION 31					
85Ω			95Ω		
AAD	Ranking of AAD	Faulty section candidate	AAD	Ranking of AAD	Faulty section candidate
0.00124	1	28	0.00095	1	29
0.00127	2	29	0.00103	2	30
<b>0.00137</b>	<b>3</b>	<b>31</b>	<b>0.00105</b>	<b>3</b>	<b>31</b>
0.00138	4	30	0.00107	4	28
0.00155	5	27	0.00137	5	27
0.00166	6	26	0.00147	6	26
0.00202	7	32	0.00155	7	32
0.00235	8	25	0.00202	8	25
0.00248	9	33	0.00204	9	33
0.00258	10	34	0.00214	10	34

 = correct answer

Although the actual fault is in the second rank, in practice, when any fault occurs, engineers have to do a physical inspection by visiting the suspected location. Hence, the proposed method reduces the high number of possibility needed to be checked.

For high impedance fault of 95Ω in the middle of section 23, section 23 gives the lowest AAD value, as shown in Table 4, which indicates the 1<sup>st</sup> rank in locating the faulty section. The faulted section was correctly identified.

### Test on section 2

For the third test, a fault is applied in the middle of section 2 with 75Ω and 95Ω fault impedance respectively. Referring to Table 5, it was found that for 75Ω, the lowest value of AAD is in section 2 while for 95Ω fault impedance, the second lowest AAD is at section 2. This shows that the proposed algorithm is capable of locating the faulty section at a branch section almost accurately.

### Test on section 31

A fault is applied in the middle of section 31 with 85Ω and 95Ω fault impedances. For both 85Ω and 95Ω fault impedances, the actual faulty section is identified from the 3<sup>rd</sup> lowest AAD as shown in Table 6. This is due to the effect of branches, high impedance fault and non-homogenous line of a distribution network that give more possibility in locating the faulty section. It is also found that the difference of AAD between the first and third lowest AAD is fairly close. Therefore, the proposed method is reasonable in locating a fault.

### Conclusion

In this work, a discrete wavelet transform-based Multi-Resolution Analysis (MRA) has been adopted to locate the faulty section in a typical 11kV distribution network system in Malaysia. The 1<sup>st</sup>, 2<sup>nd</sup> and 3<sup>rd</sup> level resolution of detailed coefficients of voltage signals have been utilized. The faulty section was determined based on the smallest value of the average of absolute difference, AAD between the measured signal and the database. The ranking of the AAD value is determined based on the lowest value to the highest value and the section with the lowest value of AAD is presumed to be the faulty section. If the fault is not found in the section with the lowest AAD value, the section with the second lowest value will be inspected. The step is repeated with increasing order of the AAD value until the actual fault is located.

The proposed algorithm has successfully determined the faulty section based on the voltage signal. Since only two cycles of post-fault voltage signal is required, this method is quick to identify the faulty section. This method has also been found to be effective in locating the faulty section and can be easily adopted.

### Acknowledgment

This work was supported by the University of Malaya, Kuala Lumpur, (UMRG grant: RG076/09AET) and under postgraduate research fund (PPP) grant (Grant code: PS009-2012A)

### Appendix

I- Line data of radial distribution network.

Section	Node		Length (km)	Type of Cable
	From	To		
1	3	4	1.254	A11UG300
2	4	14	1.29	A11UG185
3	14	17	0.5	A11UG185
4	17	18	0.5	A11UG185
5	18	19	0.25	A11UG300
6	14	15	0.395	A11UG185
7	15	16	0.51	A11UG185

8	4	5	0.14	A11UG185
9	5	6	0.4	A11UG185
10	6	7	0.35	A11UG185
11	7	12	0.3	A11UG300
12	12	13	0.75	A11UG300
13	7	8	0.2	A11UG300
14	8	9	0.5	A11UG300
15	9	10	0.27	A11UG300
16	10	11	0.5	A11UG300
17	20	34	0.5	A11UG240X
18	34	35	0.473	A11UG185
19	35	36	1.3	A11UG300
20	36	37	0.3	A11UG300
21	37	38	0.5	A11UG300
22	20	21	0.04	A11UG240X
23	21	22	0.884	A11UG185
24	22	23	0.54	A11UG185
25	23	24	0.716	A11UG240X
26	24	25	0.9	A11UG185
27	24	26	0.1	A11UG150X
28	26	27	0.5	A11UG185
29	27	28	0.723	A11UG185
30	28	29	0.45	A11UG185
31	27	30	0.594	A11UG185
32	30	31	0.908	A11UG185
33	31	32	0.5	A11UG185
34	32	33	0.5	A11UG185

II- Cable parameter

Type Of Cable	Positive Sequence (p.u/km)		Zero Sequence (p.u/km)	
	R	X	R	X
	A11UG300	0.12	0.0787	1.779
A11UG185	0.195	0.0829	2.39	0.0406
A11UG240X	0.1609	0.1524	0.1814	0.0312
A11UG150X	0.2645	0.1603	0.2960	0.0352

### REFERENCES

- [1] Kejun Mei, S.M. Rovnyak, Chee-Mun Ong, Dynamic Event Detection using Wavelet Analysis, *Power Engineering Society General Meeting, IEEE*, 2006, pp.7.
- [2] S. Bruno, M. De Benedictis, M. La Scala, Emergency Control Assessment for Mitigating the Effects of Cascading Outages, *CIGRE 2006*. <http://www.cigre.org/>
- [3] M. Bronzini, S. Bruno, M. De Benedictis, M. La Scala, Power System Modal Identification via Wavelet Analysis, *IEEE Lausanne Power Tech*, 2007, pp. 2041-2046.
- [4] S. Avdakovic, A. Nuhanovic, Identifications and Monitoring of Power System Dynamics Based on the PMUs and Wavelet Technique, *Engineering and Technology*, 2010, pp. 796-803.
- [5] S. Avdakovic, A. Nuhanovic, M. Kusljagic, M. Music, Wavelet Transform Applications in Power System Dynamics, *Electric Power Systems Research*, 2010.
- [6] W. Gao, J. Ning, Wavelet-Based Disturbance Analysis for Power System Wide-Area Monitoring, *IEEE Transactions on Smart Grid*, vol. 2, n. 1, 2011, pp. 121-130.
- [7] T. M. Lai, L. A. Snider, E. Lo, D. Sutanto, High-Impedance Fault Detection using Discrete Wavelet Transform and Frequency Range and RMS Conversion, *IEEE Transactions on Power Delivery*, vol. 20, n. 1, 2005, pp. 397-407.
- [8] A. H. Etemadi, M. Sanaye-Pasand, High-impedance Fault Detection using Multi-resolution Signal Decomposition and Adaptive Neural Fuzzy Inference System, *IET Generation, Transmission & Distribution*, vol. 2, n. 1, 2008, p. 110.
- [9] M. Michalik, M. Lukowicz, W. Rebizant, S.-J. Lee, S.-H. Kang, Verification of the Wavelet-Based HIF Detecting Algorithm Performance in Solidly Grounded MV Networks, *IEEE Transactions on Power Delivery*, vol. 22, n. 4, 2007, pp. 2057-2064.
- [10] M. Sarlak, S. M. Shahrtash, High Impedance Fault Detection using Combination of Multi-layer Perceptron Neural Networks Based on Multi-resolution Morphological Gradient Features of Current Waveform, *IET Generation, Transmission & Distribution*, vol. 5, n. 5, 2011, p. 588.
- [11] M. Mirzaei, M. Z. A. A. Kadir, E. Moazami, H. Hizam, Review of Fault Location Methods for Distribution Power System,

- Australian Journal of Basic and Applied Sciences* vol. 3, n. 3, 2009, pp. 2670-2676.
- [12] T. Short, J. Kim, C. Melhorn, Update on Distribution System Fault Location Technologies and Effectiveness, *20th International Conference and Exhibition on Electricity Distribution - Part 1*, pp. 1-4, 2009.
- [13] J. Mora, J. Meléndez, M. Vinyoles, J. Sánchez, M. Castro, An Overview to Fault Location Methods in Distribution System Based on Single End Measures of Voltage and Current, *ICREPQ'04 – International Conference on Renewable Energy and Power Quality*, 2004.
- [14] N. I. Elkalashy, M. Lehtonen, H. A. Darwish, A.-M. I. Taalab, M. A. Izzularab, A Novel Selectivity Technique for High Impedance Arcing Fault Detection in Compensated MV Networks, *European Transactions on Electrical Power*, vol. 18, n. 4, 2008, pp. 344-363.
- [15] N. I. Elkalashy, M. Lehtonen, H. A. Darwish, A.-M. I. Taalab, M. A. Izzularab, DWT-based Extraction of Residual Currents Throughout Unearthed MV Networks for Detecting High-impedance Faults Due to Leaning Trees, *European Transactions on Electrical Power*, vol. 17, n. 6, 2007, pp. 597-614.
- [16] U. D. Dwivedi, S. N. Singh, S. C. Srivastava, A Wavelet Based Approach for Classification and Location of Faults in Distribution Systems, *Annual IEEE India Conference*, pp. 488-493, 2008.
- [17] L. Garcia-Santander, P. Bastard, M. Petit, I. Gal, E. Lopez, H. Opazo, Down-conductor Fault Detection and Location Via a Voltage Based Method For Radial Distribution Networks, *IEE Proceedings - Generation, Transmission and Distribution*, vol. 152, n. 2, 2005, p. 180.
- [18] Z.-Y. Li, W.-I. Wu, Classification of Power Quality Combined Disturbances Based on Phase Space Reconstruction and Support Vector Machines, *Journal of Zhejiang University - Science A*, vol. 9, 2008, pp. 173-181.
- [19] S. Chen, Feature Selection For Identification and Classification of Power Quality Disturbances, *Power Engineering Society General Meeting*, Vol. 3, 2005, pp. 2301-2306.
- [20] P. K. Dash, B. K. Panigrahi, G. Panda, Power Quality Analysis using S-transform, *IEEE Transactions on Power Delivery*, vol. 18, 2003, pp. 406-411.
- [21] T. K. Abdel-Galil, E. F. El-Saadany, A. M. Youssef, M. M. A. Salama, Disturbance Classification using Hidden Markov Models and Vector Quantization, *IEEE Transactions on Power Delivery*, vol. 20, 2005, pp. 2129-2135.
- [22] S. Suja, J. Jerome, Pattern Recognition of Power Signal Disturbances using S-Transform and TT-Transform, *International Journal of Electrical Power & Energy Systems*, vol. 32, 2010, pp. 37-53.
- [23] H. Mokhlis, Hasmaini Mohamad, A.H.A Bakar, H.Y.Li, Evaluation of Fault Location based on Voltage Sags Profiles: a Study on the Influence of Voltage Sags Patterns, *International Review of Electrical Engineering (IREE)*, vol. 6, n.2, March-April 2011, pg 874-880.

**Authors:** Mohd Syukri Ali, University of Malaya, 59200 Kuala Lumpur, E-mail: [mosba86@yahoo.com.my](mailto:mosba86@yahoo.com.my). Dr Ab Halim Abu Bakar, University of Malaya, 59200 Kuala Lumpur, E-mail: [a.halim@um.edu.my](mailto:a.halim@um.edu.my). Dr Hazlie Mokhlis, University of Malaya, 59200 Kuala Lumpur, E-mail: [hazli@um.edu.my](mailto:hazli@um.edu.my). Dr Hamzah Arof, University of Malaya, 59200 Kuala Lumpur, E-mail: [ahamzah@um.edu.my](mailto:ahamzah@um.edu.my). Dr Hazlee Azil Illias, University of Malaya, 59200 Kuala Lumpur, E-mail: [h.illias@um.edu.my](mailto:h.illias@um.edu.my)